Journal of the Egyptian Mathematical Society (2016) **24**, 116–124

Egyptian Mathematical Society

Journal of the Egyptian Mathematical Society

www.etms-eg.org
www.elsevier.com/locate/joems

ORIGINAL ARTICLE

Numerical study of shock waves in non-ideal magnetogasdynamics (MHD)

Addepalli Ramu *, **Narsimhulu Dunna, Dipak Kumar Satpathi**

Department of Mathematics, BITS-Pilani, Hyderabad Campus, India

Received 24 February 2014; revised 30 August 2014; accepted 21 October 2014
Available online 11 February 2015

KEYWORDS

Similarity solutions;
Shock waves;
Magnetogasdynamics;
Rankine–Hugoniot condition;
Mie–Gruneisen type;
Numerical solution

Abstract One-dimensional unsteady adiabatic flow of strong converging shock waves in cylindrical or spherical symmetry in MHD, which is propagating into plasma, is analyzed. The plasma is assumed to be non-ideal gas whose equation of state is of Mie–Gruneisen type. Suitable transformations reduce the governing equations into ordinary differential equations of Poincare type. In the present work, McQueen and Royce equations of state (EOS) have been considered with suitable material constants and the spherical and cylindrical cases are worked out in detail to investigate the behavior and the influence on the shock wave propagation by energy input and $\beta(\rho/\rho_0)$, the measure of shock strength. The similarity solution is valid for adiabatic flow as long as the counter pressure is neglected. The numerical technique applied in this paper provides a global solution to the implosion problem for the flow variables, the similarity exponent α for different Gruneisen parameters. It is shown that increasing $\beta(\rho/\rho_0)$ does not automatically decelerate the shock front but the velocity and pressure behind the shock front increases quickly in the presence of the magnetic field and decreases slowly and become constant. This becomes true whether the piston is accelerated, is moving at constant speed or is decelerated. These results are presented through the illustrative graphs and tables. The magnetic field effects on the flow variables through a medium and total energy under the influence of strong magnetic field are also presented.

MATHEMATICS SUBJECT CLASSIFICATION (MSC): 76M55; 76L05; 76W05

1. Introduction

Shock processes occur naturally in various astrophysical situations such as supernova explosions, photo-ionized gas, stellar winds, and collisions between high velocity clumps of interstellar gas. Magnetogasdynamics applies to many conductive fluid and plasma flows encountered in nature. In several circumstances, the flow is subject to a strong as well as a weak magnetic field. Such situation can be thought

* Corresponding author.
Peer review under responsibility of Egyptian Mathematical Society.

ELSEVIER Production and hosting by Elsevier

http://dx.doi.org/10.1016/j.joems.2014.10.002

of occurring in earth's liquid core, and is present in solar physics such as sunspots, solar flares, solar corona, and solar winds. The strong magnetic fields play significant roles in the dynamics of the interstellar medium. A theoretical study of the imploding shock wave near the center of convergence, in an ideal gas was first investigated by Guderley [1]. Several authors contributed to this investigation and we mention the contributions of, Hafner [2], Manganaro and Oliveri [3], Sharma and Radha [4], Hunter and Ali [5], Sharma and Arora [6], Stanyukovich [7], Chisnell [8], Lazarus and Richtmyer [9], Ramu and Ranga Rao [10], Madhumita and Sharma [11], Sen [12], who presented high accuracy results and alternative approaches for the investigation of implosion problem. The propagation of shock waves under the influence of strong magnetic field is of great interest to many researchers in various fields such as astrophysics, nuclear science, geophysics, and plasma physics. MHD shock waves in perfect gas are under extensive exploration and attained good attention in the past decades. Propagation of shock waves in magneto hydrodynamics (MHD) has been studied by several researchers. De Hoffmann and Teller [13] developed a mathematical treatment for the motion of MHD shock waves in the very weak and very strong magnetic fields. Bazer and Ericson [14] were first among the many researchers to study the hydromagnetic shocks for astrophysical applications and analytical solutions were presented by Genot [15] for anisotropic MHD shocks. A number of approaches namely, the similarity method, power series solution method, CCW method have been used for the theoretical investigations of MHD shock waves in homogeneous and inhomogeneous media.

In the recent years much attention has been focused on the self-similar solutions using similarity transformations because of their wide applications in determining solutions of nonlinear differential equations of physical interest. The gas attains very high temperature due to the propagation of shock waves and at such a high temperature, the gas gets ionized, hence effects of magnetic field become significant in the study of converging shock waves. The study of MHD shock waves in a non-ideal gas is of great scientific interest in many problems because of their applications in the areas of astrophysics, oceanography, atmospheric sciences, hypersonic aerodynamics and hypervelocity impact.

In this paper a model to determine the similarity solutions to the problem of gas dynamic flow under the influence of strong magnetic field is presented. The problem treated here involves distinct features: the global behavior of the physical parameter has been studied; the initial pressure ratio is confined to a moderate value. The path of the piston is imposed as boundary condition. Thus an accelerated, a decelerated or a constant velocity piston can be specified. Self-similarity requires the velocity of shock and the velocity of piston to be proportional to some power law $R(t) \propto (t)^{\alpha}$ where $R(t)$ is the position of the shock wave front from the center at time t and α is the similarity exponent. The numerical values of similarity exponents and profiles of flow variables are obtained. These are presented through the illustrative graphs and tables. The magnetic field effects on the flow variables through a medium and total energy under the influence of strong magnetic field are also presented.

2. Basic equations and boundary conditions

The non-steady one dimensional flow is a function of two independent variables the time t and the space coordinate r. The conservation equations governing the flow can be written as [12,16–20]

$$\frac{\partial \rho}{\partial t} + u\frac{\partial \rho}{\partial r} + \rho\frac{\partial u}{\partial r} + \frac{(m-1)\rho u}{r} = 0 \tag{1}$$

$$\frac{\partial u}{\partial t} + u\frac{\partial u}{\partial r} + \rho^{-1}\left(\frac{\partial p}{\partial r} + \frac{\partial h}{\partial r}\right) = 0 \tag{2}$$

$$\frac{\partial p}{\partial t} + u\frac{\partial p}{\partial r} - a^2\left(\frac{\partial \rho}{\partial t} + u\frac{\partial \rho}{\partial r}\right) = 0 \tag{3}$$

$$\frac{\partial h}{\partial t} + u\frac{\partial h}{\partial r} + 2h\frac{\partial u}{\partial r} + 2h(m-1)u/r = 0 \tag{4}$$

where $\rho(r,t)$, $u(r,t)$ and $p(r,t)$ denote the density, velocity, and pressure of the gas particles behind the shock front, $h(r,t)$ is the magnetic pressure defined by $h = \frac{\mu H^2}{2}$ with μ as magnetic permeability and H is the transverse magnetic field, $a^2 = (\Gamma + 1)p/\rho$ is the equilibrium speed of sound, Γ is the Gruneisen coefficient, $m = 2(3)$ denote shock wave in cylindrical (spherical) geometry.

It is assumed that the plasma has infinite electrical conductivity and permeated by an axial magnetic field orthogonal to the trajectories of the gas particles. Shock is assumed to be strong and propagating into a medium according to a power law $R(t) \propto (t)^{\alpha}$, where $R(t)$ is the position of the shock wave front from the center at time t and $t = 0$ corresponds to the instant of the convergence when $R = 0$. The equation of state under equilibrium condition is of Mie–Gruneisen type [10],

$$\mathrm{p} = \rho e \Gamma(\rho/\rho_0) \tag{5}$$

where the function $\Gamma(\rho/\rho_0)$ is the Gruneisen parameter.

2.1. Boundary conditions

The boundary conditions at shock front due to Rankine–Hugoniot, can be written as [7,18,20]

$$\rho = \frac{\Gamma+2}{\Gamma}\rho_0\left(1 + \frac{2}{\Gamma}\left(\frac{\mathrm{a_0}}{\mathrm{D}}\right)^2\right) \quad u = \frac{2}{\Gamma+2}D\left(1 - \frac{a_0}{D}\right) \tag{6}$$

$$\mathrm{p} = \frac{2}{\Gamma+2}\rho_0 D^2\left\{1 - \frac{\Gamma}{2}\left(\frac{a_0}{D}\right)^2\right\} - \frac{1}{2}\frac{(\Gamma+2)^2}{\Gamma^2}C_0\rho_0 D^2\left\{1 + \frac{2}{\Gamma}\left(\frac{a_0}{D}\right)^2\right\}^2 \tag{7}$$

$$\mathrm{h} = \frac{1}{2}\left(\frac{\Gamma+2}{\Gamma}\right)^2 C_0\rho_0 D^2\left\{1 + \frac{2}{\Gamma}\left(\frac{a_0}{D}\right)^2\right\}^2 \tag{8}$$

where $C_0 = \frac{2h_0}{\rho_0 D^2}$ is the shock Cowling number and D is the speed of the shock wave defined as $D = \frac{dR}{dt}$, since the initial energy input E_0 of explosion is very large, the shocks speed $D \gg a_0$ so that $\frac{a_0}{D} \to 0$ in the strong shock limit.

Therefore the Rankine–Hugoniot jump conditions (6)–(8) in the case of strong shock waves can be written as

$$\rho = \frac{\Gamma+2}{\Gamma}\rho_0 \qquad u = \frac{2}{\Gamma+2}D \tag{9}$$

$$p = \frac{2}{\Gamma+2}\rho_0 D^2 - \frac{1}{2}\frac{(\Gamma+2)^2}{\Gamma^2}C_0\rho_0 D^2 \tag{10}$$

$$h = \frac{1}{2}\frac{(\Gamma+2)^2}{\Gamma^2}C_0\rho_0 D^2 \tag{11}$$

Using Eqs. (9)–(11), the EOS (5) can be written as [10]

$$\left(2-\frac{C_0\beta^3}{(\beta-1)}\right)=(\beta-1)\Gamma(\beta) \tag{12}$$

where $\beta(\rho/\rho_0)$ is the compression just behind the shock, which is called measure of shock strength. When $C_0 = 0$, the propagation of shock wave into a medium is without magnetic field and Eq. (12) reduces to the non-magnetic case in a non-ideal medium. The total energy E inside a blast wave is equal to the energy supplied by the explosive and thus constant. The total energy is given by the expression

$$E=4\pi\int_0^D\left(\frac{1}{2}\rho u^2+\frac{p}{\Gamma}+h\right)R^{(m-1)}dR \tag{13}$$

Eliminating ρ_0 from Eqs. (10) and (11), p and h can be written as (after using (9))

$$p=\frac{\Gamma}{2}\rho u^2-\frac{C_0}{8}\frac{(\Gamma+2)^3}{\Gamma}\rho u^2 \qquad h=\frac{1}{8}\frac{(\Gamma+2)^3}{\Gamma}C_0\rho u^2$$

2.2. Conservation equations and boundary conditions

The basic equations can be made dimensionless by transforming the independent variables for space r and time t in to new independent variables as follows [18]

$$p=\frac{\Gamma}{2}\rho u^2-\frac{C_0}{8}\frac{(\Gamma+2)^3}{\Gamma}\rho u^2 \qquad h=\frac{1}{8}\frac{(\Gamma+2)^3}{\Gamma}c_0\rho u^2 \tag{14}$$

$$\rho=\rho_0 G(\xi) \tag{15}$$

$$u=DV(\xi) \tag{16}$$

similarity variable $\xi=\left(\frac{r}{R}\right)$

The transformed system of three ordinary differential equations in non-dimensional form depend only on the similarity variable ξ and are,

$$\{(1+\Gamma)V-\xi\}\left(\frac{V'}{V}\right)+\frac{\Gamma V}{2}\left(\frac{G'}{G}\right)-\frac{(\Gamma+2)V}{2R}\left(\frac{G'}{G}\right)^2=-\lambda \tag{17}$$

$$\left\{\left(1+\frac{\Gamma}{2}\right)V-\xi\right\}\left(\frac{V'}{V}\right)-\frac{\Gamma\phi(\Gamma)}{R}(V+\xi^2D)\left(\frac{G'}{G}\right)^2=-\lambda-\frac{\Gamma V(m-1)}{2\xi} \tag{18}$$

$$\left(\frac{3V}{2}-\xi\right)\left(\frac{V'}{V}\right)-\frac{(\Gamma-1)}{\Gamma R}(V+\xi^2D)\left(\frac{G'}{G}\right)^2=-\lambda-\frac{(m-1)V}{2\xi} \tag{19}$$

where D is $\frac{dR}{dt}=\dot{R},\lambda=\dot{D}\frac{R}{D^2},G,V$ are new dimensionless functions of density (ρ) and velocity (u). Further using Eq. (17), the Eqs. (18) and (19) can be reduced into a system of two ordinary differential equations.

$$A_1\left(\frac{G'}{G}\right)+B_1\left(\frac{V'}{V}\right)=C_1 \tag{20}$$

$$A_2\left(\frac{G'}{G}\right)+B_2\left(\frac{V'}{V}\right)=C_2 \tag{21}$$

The above equations can be written in matrix form as

$$\begin{bmatrix}A_1 & B_A\\ A_2 & B_2\end{bmatrix}\begin{bmatrix}\frac{G'}{G}\\ \frac{V'}{V}\end{bmatrix}=\begin{bmatrix}C_1\\ C_2\end{bmatrix} \tag{22}$$

where

$$A_1=\frac{(V+\xi^2D)\Gamma^2\phi(\Gamma)}{\Gamma+2},\quad A_2=\frac{(V+\xi^2D)(\Gamma-1)}{\Gamma+2},$$

$$B_1=\frac{2\{1+\Gamma)V-\xi\}}{\Gamma V}A_1-\frac{1}{2}\{(2+\Gamma)V-2\xi\}$$

$$B_2=\frac{2\{1+\Gamma)V-\xi\}}{\Gamma V}A_2-\frac{1}{2}(3V-2\xi),$$

$$C_1=\left(1-\frac{2}{\Gamma V}A_1\right)\lambda+\frac{\Gamma V(m-1)}{2\xi}$$

$$C_2=\left(1-\frac{2}{\Gamma V}A_2\right)\lambda+\frac{V(m-1)}{2\xi},$$

$$\phi(\Gamma)=\frac{2(\Gamma+2)\Gamma^2-c_0(\Gamma-1)(\Gamma+2)^3}{4\Gamma^4-c_0\Gamma^2(\Gamma+2)^3},$$

$$G'=\mathrm{G}\frac{\Delta_1}{\Delta}\quad \mathrm{V}'=\mathrm{V}\frac{\Delta_2}{\Delta} \tag{23}$$

and

$$\Delta=\frac{(V-\alpha\xi^2)}{f_3}\left[\frac{V}{2}f_1+6\xi f_2\right]$$

$$\Delta_1=\frac{1}{\Gamma f_3}\left[(V-\alpha\xi^2)\left\{\lambda f_4+(m-1)\left(1+\frac{V}{\xi}(\Gamma+1)\right)f_5\right\}+\frac{V}{2}f_6\left\{\lambda+(m-1)\left(1-\frac{V}{\xi}\right)\right\}\right]$$

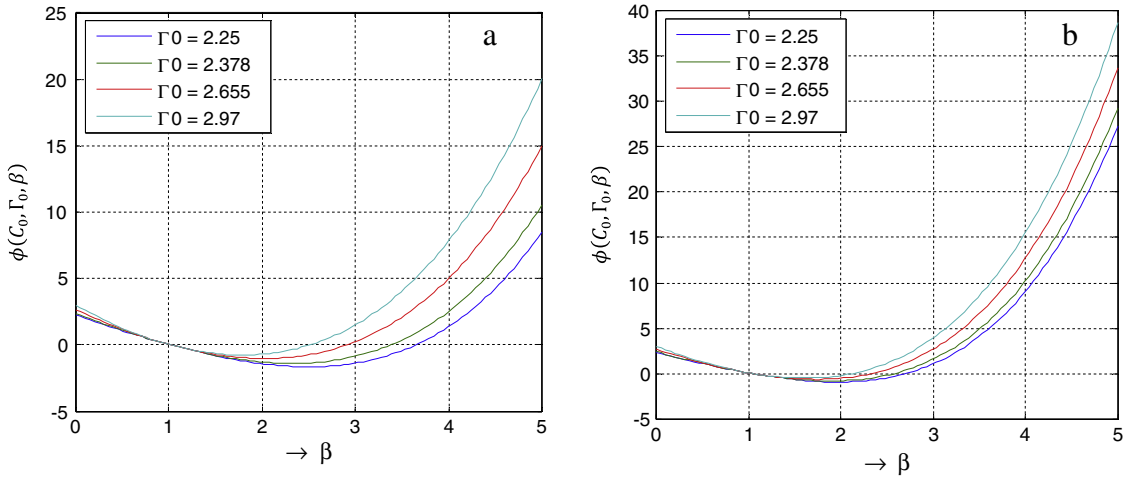

Figure 1 Graphical approach to estimate positive roots of equation $\phi(C_0,\Gamma_0,\beta)=0$ in the case of McQueen EOS, when (a) $C_0 = 0.02$ and (b) $C_0 = 0.05$.

$\Delta_2 = \frac{(V-\alpha\xi^2)}{f_3}\left[6\lambda f_7 - \frac{(m-1)V}{2\xi} f_5\right]$, ($f_1$, f_2, f_3, f_4, f_5, f_6, and f_7 are functions of Γ)

$$f_1(\Gamma) = 2\Gamma^2(2\Gamma^2 - \Gamma - 10) - C_0\Gamma^2(\Gamma^5 + 4\Gamma^4 + \Gamma^3 - 10\Gamma^2 - 4\Gamma + 8),$$

$$f_2(\Gamma) = \Gamma^4(4-\Gamma), \quad f_3(\Gamma) = 4\Gamma^2(\Gamma+2) - C_0(\Gamma+2)^4,$$

$$f_4(\Gamma) = 2(-5\Gamma^3 + 4\Gamma^2 - \Gamma - 10) - \frac{1}{\Gamma^2} f_1,$$

$$f_5(\Gamma) = 4\Gamma^3(\Gamma-4) - f_4, \quad f_6(\Gamma) = \Gamma(\Gamma-1)(\Gamma+2) f_3,$$

$$f_7(\Gamma) = \frac{1}{\Gamma^2} f_2 \text{ and } \lambda = 1 - \frac{1}{\alpha}$$

The transformed boundary conditions are $G(1) = \beta$ and $V(1) = 1 - \frac{1}{\beta}$

3. Solution procedure

3.1. Evaluation of $\beta(\rho/\rho_0)$ the measure of shock strength

Considering the EOS of Mie–Gruneisen type [10]:

(a) The McQueen defined by

$$\Gamma(G) = \frac{\Gamma_0}{G} \quad \text{and} \tag{24}$$

(b) The Royce EOS defined by

$$\Gamma(G) = \Gamma_0 - b\left(1 - \frac{1}{G}\right) \tag{25}$$

along with Eq. (12) we obtain bi-quadratic equations in β as

$$c_0\beta^4 + (\Gamma_0 - 2)\beta^2 + 2(1-\Gamma_0)\beta + \Gamma_0 = 0 \tag{26}$$

and

$$c_0\beta^4 + (\Gamma_0 - b)\beta^3 + (3b - 2 - 2\Gamma_0)\beta^2 + (2 - 3b + \Gamma_0)\beta + b = 0 \tag{27}$$

respectively. These equations are solved to obtain a unique value of β corresponding to the constants C_0,Γ_0 and b. According to Descartes's rule of signs these two equations will have at least two real and two complex roots. This was found to be true as can be seen from the solution curves and from these solutions curves (Figs. 1 and 2) it is observed that irrespective of the constants a real root is always $\beta = 1$ and this corresponds to the case where magnetic effect $C_0 = 0$. Neglecting the imaginary roots the other roots are solved numerically using MATLAB and are tabulated in Tables 1 and 2.

3.2. Numerical integration solution procedure

In order to integrate the set of non-linear ordinary differential Eq. (23), we use Runge–Kutta fourth order method with a small step size. The integration is carried out in the range, $1 \leqslant \xi < \infty$. Starting the integration with a known value of β and α (α is evaluated corresponding to every β iteratively), shown in Tables 1 and 2. The whole solution procedure is repeated until the shock conditions are satisfied within the desired accuracy.

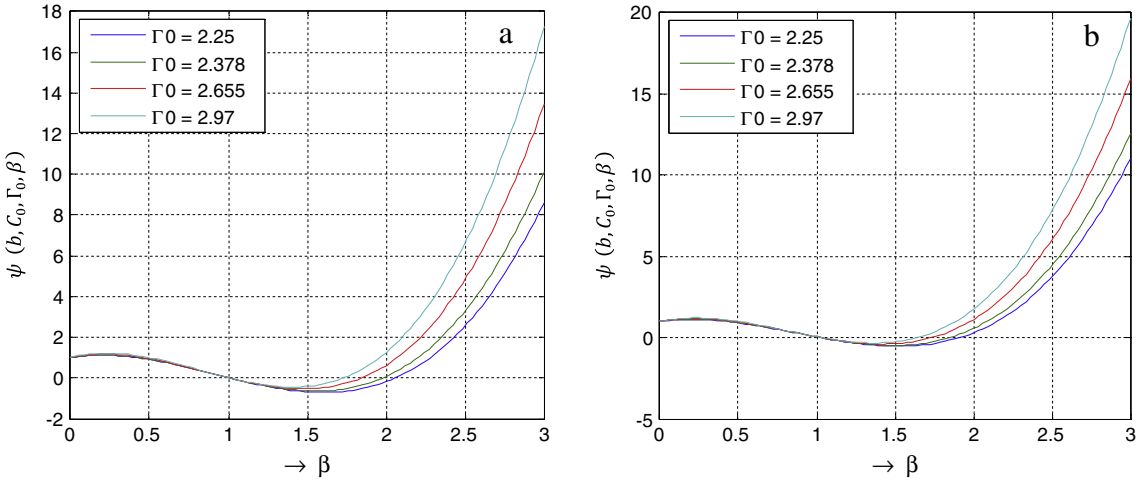

Figure 2 Graphical approach to estimate positive roots of equation $\psi(b, C_0, \Gamma_0, \beta) = 0$ in the case of Royce EOS, when (a) $C_0 = 0.02$ and (b) $C_0 = 0.05$.

Table 1 Selected values of β and α for McQueen EOS for different values of C_0.

Γ_0	$C_0 = 0.02$		$C_0 = 0.05$	
	β	α	β	α
2.25	3.64832	0.72590123673362	2.70724	0.63062011495102
2.378	3.38294	0.704399132115852	2.58037	0.612458678406585
2.655	2.90851	0.656181343712072	2.34205	0.573023633141906
2.97	2.51656	0.602632164542073	2.12633	0.529706113350233

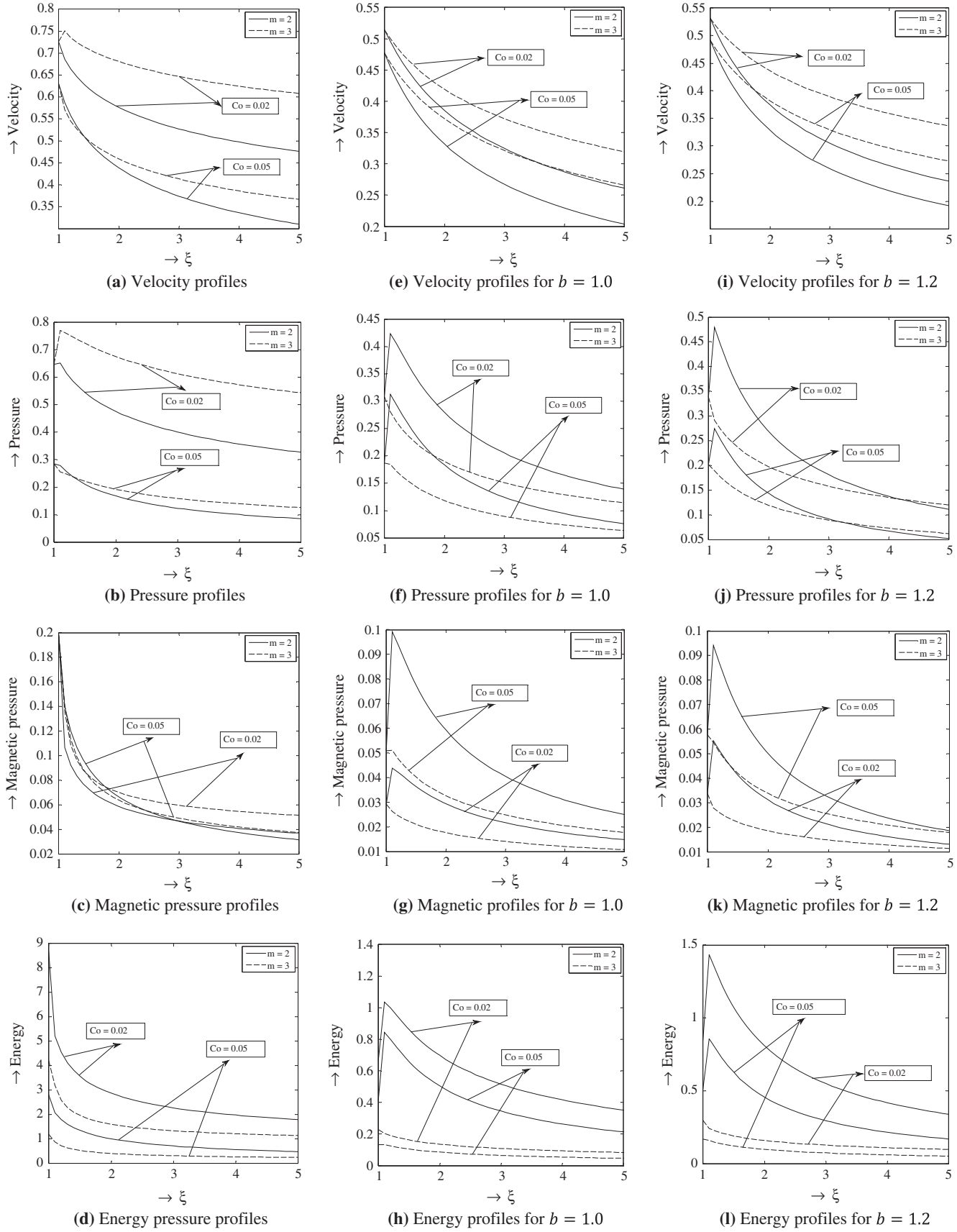

(a) Velocity profiles **(e)** Velocity profiles for $b = 1.0$ **(i)** Velocity profiles for $b = 1.2$

(b) Pressure profiles **(f)** Pressure profiles for $b = 1.0$ **(j)** Pressure profiles for $b = 1.2$

(c) Magnetic pressure profiles **(g)** Magnetic profiles for $b = 1.0$ **(k)** Magnetic profiles for $b = 1.2$

(d) Energy pressure profiles **(h)** Energy profiles for $b = 1.0$ **(l)** Energy profiles for $b = 1.2$

Figure 3 (a–d) Represents flow profiles of McQueen EOS for different values of C_0; (e–h) represents flow profiles of Royce EOS for $b = 1.0$, and different values of C_0; (i–l) represents flow profiles of Royce EOS for $b = 1.2$, and different values of C_0 (in all figures $\Gamma_0 = 2.25$).

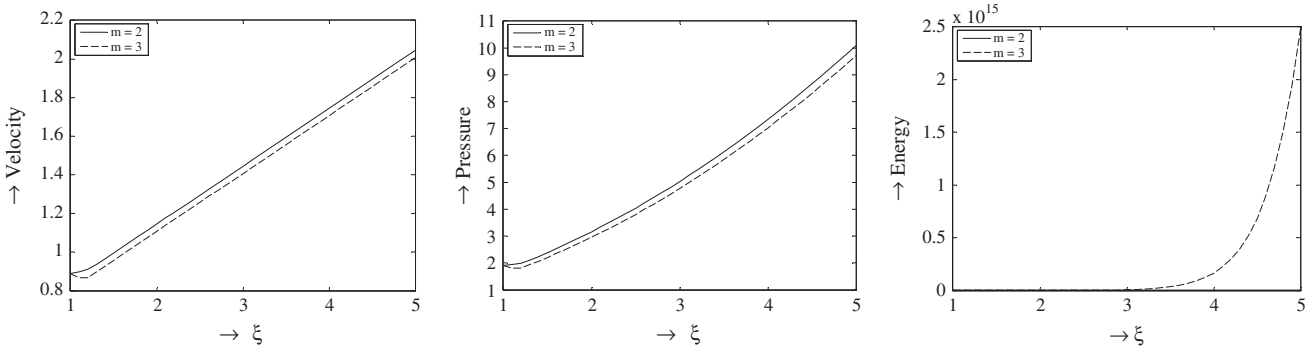

(a) Velocity profiles **(b)** Pressure profiles **(c)** Energy profiles

Figure 4 Flow profiles of McQueen EOS for $\Gamma_0 = 2.25$, magnetic effect $C_0 = 0$, and $m = 2,\ 3$.

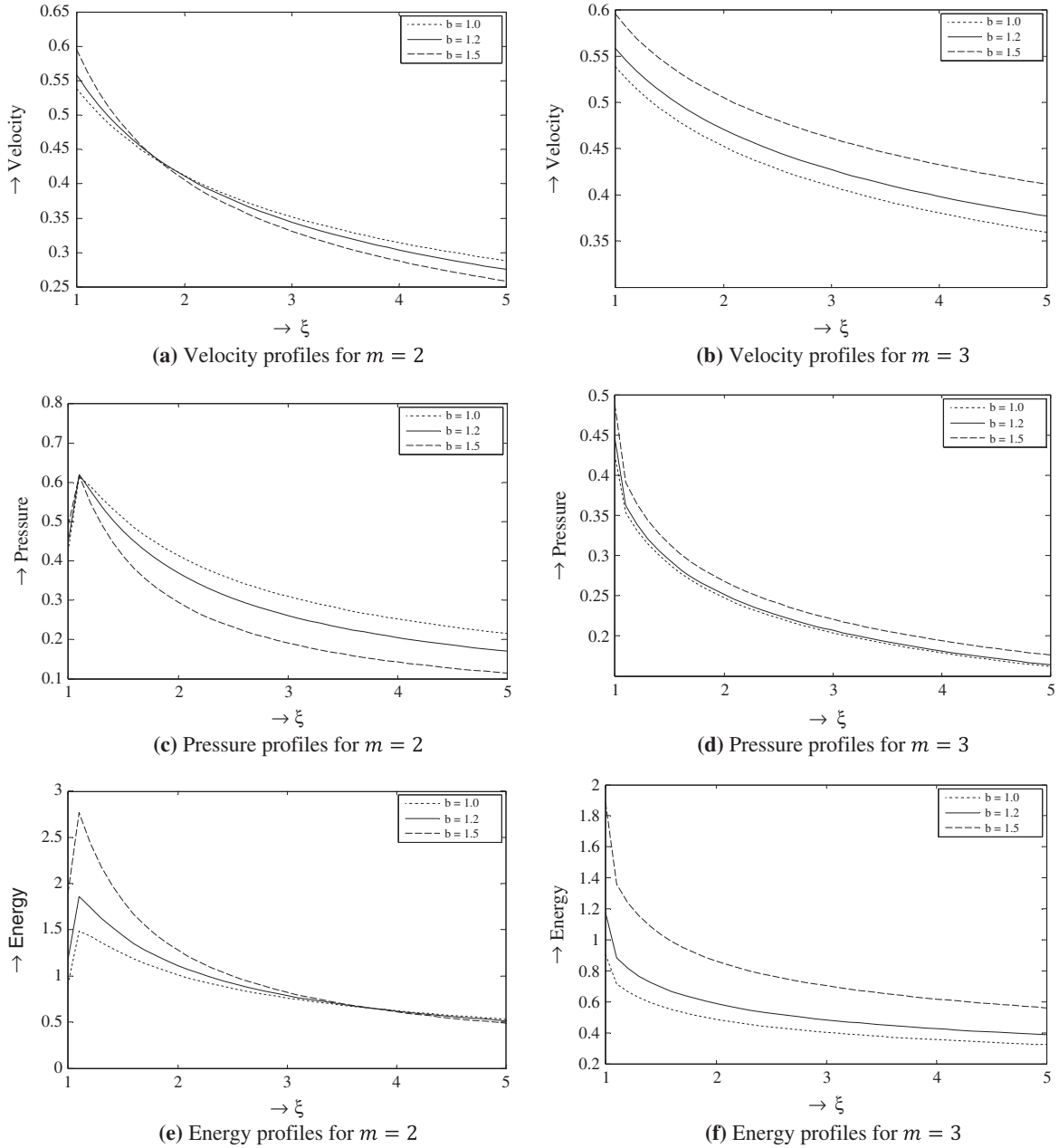

(a) Velocity profiles for $m = 2$

(b) Velocity profiles for $m = 3$

(c) Pressure profiles for $m = 2$

(d) Pressure profiles for $m = 3$

(e) Energy profiles for $m = 2$

(f) Energy profiles for $m = 3$

Figure 5 Flow profiles of Royce EOS for $\Gamma_0 = 2.25$, $C_0 = 0$, and different values of b.

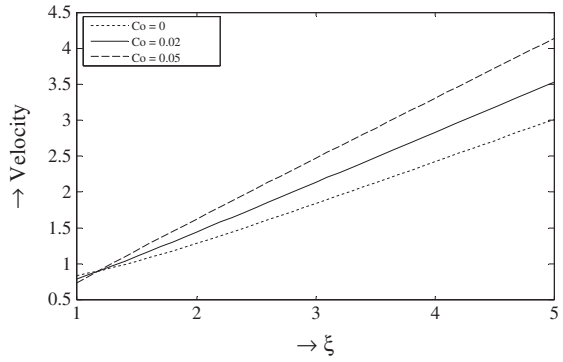

(a) Velocity profiles for $m = 2$

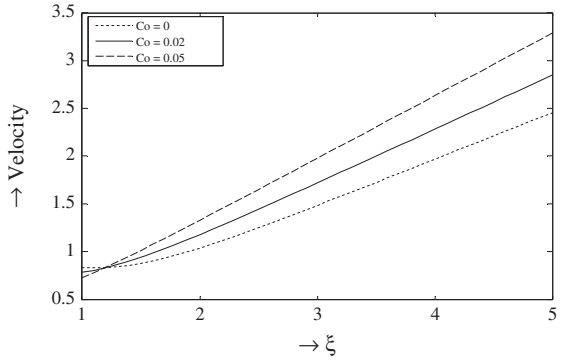

(b) Velocity profiles for $m = 3$

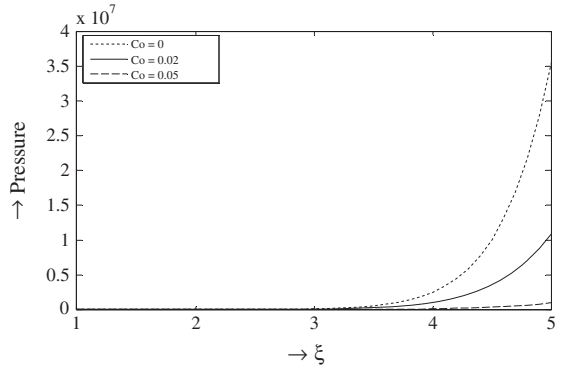

(c) Pressure profiles for $m = 2$

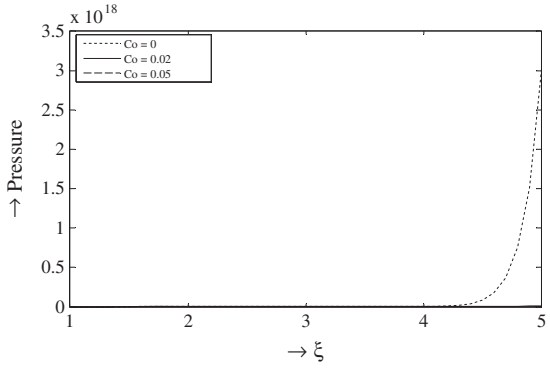

(d) Pressure profiles for $m = 3$

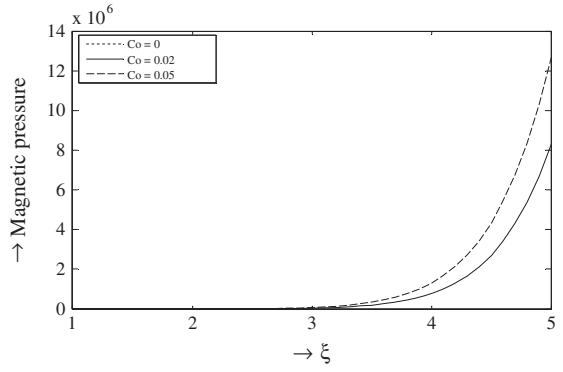

(e) Magnetic pressure profiles for $m = 2$

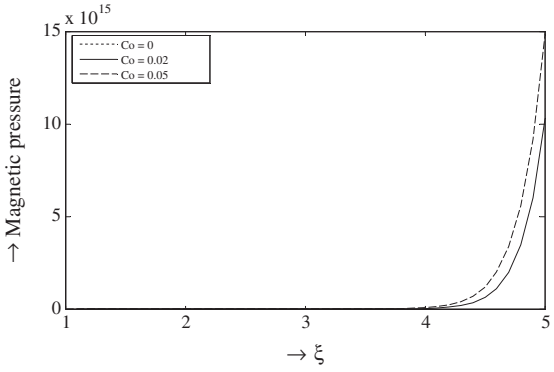

(f) Magnetic pressure profiles for $m = 3$

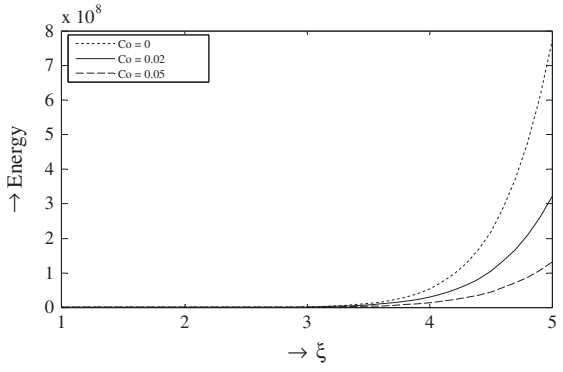

(g) Energy profiles for $m = 2$

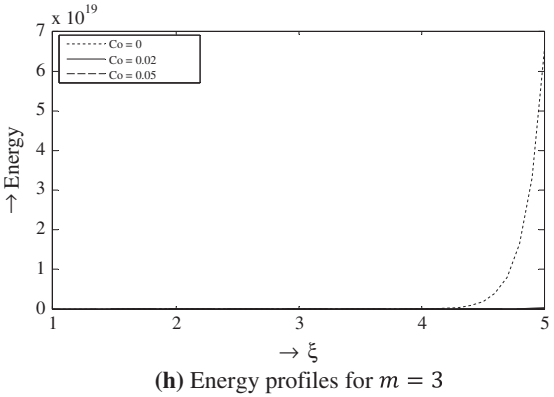

(h) Energy profiles for $m = 3$

Figure 6 Flow profiles of perfect gas EOS for $\Gamma = 1.4$ and different values of C_0.

Table 2 Selected values of β and α for Royce EOS for different values of C_0 and an arbitrary constant b.

Γ_0	C_0	$b = 1$		$b = 1.2$		$b = 1.5$	
		β	α	β	α	β	α
2.25	0	2.16886	0.538928284905434	2.26621	0.558734627417583	2.47481	0.595928576335153
	0.02	2.05713	0.513885850675456	2.13416	0.531431570266522	2.29118	0.563543676184324
	0.05	1.91188	0.476954620582882	1.96778	0.491813109189035	2.07584	0.518267303838446
2.378	0	2.07536	0.518155886207694	2.15239	0.535400183052328	2.30928	0.566964595025289
	0.02	1.97778	0.494382590581359	2.03990	0.509779891171136	2.16171	0.537403259456634
	0.05	1.84825	0.458947653185446	1.89427	0.472092151594018	1.98075	0.495140729521646
2.655	0	1.91908	0.478916981053421	1.96875	0.492063492063492	2.06256	0.515165619424405
	0.02	1.84246	0.457247375791062	1.88369	0.469127085666962	1.95978	0.489738644133525
	0.05	1.73720	0.424361040755238	1.76876	0.434632171690902	1.82537	0.452165862263541
2.97	0	1.79103	0.441662060378665	1.82373	0.451673219171698	1.88226	0.468723768236057
	0.02	1.72918	0.421691206236482	1.75691	0.430818880876084	1.80579	0.446225751610099
	0.05	1.64179	0.390908703305539	1.66354	0.398872284405545	1.70115	0.412162360755959

4. Results and discussion

In this paper, the entire computational work has been carried out using MATLAB. Numerical calculations are performed for the values of non-ideal parameters $C_0 = 0.02,\ 0.05$; $b = 1.0,\ 1.2,\ 1.5,\ 2.25$ and $\Gamma_0 = 2.25,\ 2.378,\ 2.655,\ 2.97$. The values of similarity exponent α for different values of C_0 in the case of McQueen EOS and Royce EOS are listed in Tables 1 and 2 respectively. The variations of non-dimensional shock velocity, pressure, magnetic pressure and energy deposition with ξ for McQueen EOS are shown in Fig. 3(a)–(d). It is observed that the flow variables Velocity, Pressure (for both cylindrical and spherical geometry) are high at the shock front (for the McQueen EOS) and increases with the increase in the non-idealness parameters and reduce gradually as ξ increases. Again from Fig. 3(c) and (d) at $\xi = 1$, magnetic pressure and energy are very high and reduce drastically with increase in ξ and become constant. Also from Fig. 3(e)–(l) for Royce EOS it can be seen that the velocity, pressure, magnetic pressure and energy profiles, first increase with the increase in ξ and decrease with further increase in ξ. It is notable that increase in the non-idealness parameters (from Tables 1 and 2) have effect on β. As β value increases, increase in velocity, pressure, magnetic pressure and energy is prominent for both the EOS. Thus it is observed from Fig. 3(e)–(l) that increase in β does not automatically decelerate the shock front but the velocity and pressure behind the shock front increases quickly in the presence of the magnetic field and decrease slowly and become constant. Also in the presence of non-idealness parameters and in the absence of magnetic field the velocity and pressure profiles reduce gradually. It is noted from Fig. 4(a)–(d) for the EOS of McQueen, density and energy increase drastically for $\xi > 2.5$ whereas with non-idealness parameters the velocity and pressure increase sharply for $\xi \geqslant 1$. From Fig. 5(a)–(f) with non-idealness parameters in the absence of magnetic field (C_0) for the Royce EOS the velocity and pressure profiles gradually decrease (see Fig. 5(a) and (d)) and become constant, whereas pressure and energy profiles (see Fig. 5(b), (c), (e), and (f)) initially increase with the increase in ξ and reduce slowly with increasing ξ and become constant. Also from Fig. 6(a)–(e) it is observed that shock propagates more rapidly in perfect gas in presence of the magnetic field. It is interesting to note that the rate of rise in the flow variables increase with the increase in the strength of magnetic field.

5. Conclusions

In this paper, the variations of non-dimensional shock velocity, pressure, magnetic pressure and energy deposition with ξ for both EOS are presented. The entire computational work has been carried out using MATLAB for the values of non-ideal parameters $C_0 = 0.02,\ 0.05$; $b = 1.0,\ 1.2,\ 1.5,\ 2.25$ and $\Gamma_0 = 2.25,\ 2.378,\ 2.655,\ 2.97$. The values of similarity exponent α for different values of C_0 in the case of McQueen EOS and Royce EOS are evaluated. The results of the study can be summarized as follows.

1. The flow variables Velocity, Pressure for both cylindrical and spherical geometry are high at the shock front for the McQueen EOS increases with the increase in the non-idealness parameters and reduce gradually as ξ increases.
2. At $\xi = 1$, magnetic pressure and energy are very high and reduce drastically with increase in ξ and become constant. The velocity, pressure, magnetic pressure and energy profiles, first increase with ξ and then decrease with further increase in ξ for Royce EOS.
3. It is notable that increase in the non-idealness parameters has effect on β. Increase in β does not automatically decelerate the shock front but the velocity and pressure behind the shock front increases quickly in the presence of the magnetic field and decrease slowly and become constant.
4. In the presence of non-idealness parameters and in the absence of magnetic field the velocity and pressure profiles reduce gradually. In the EOS of McQueen, density and energy increase drastically for $\xi > 2.5$ whereas with non-idealness parameters the velocity and pressure increase sharply for $\xi \geqslant 1$.
5. With non-idealness parameters in the absence of magnetic field (C_0) for the Royce EOS the velocity and pressure profiles gradually decrease and become constant, whereas pressure and energy profiles initially increase with the increase in ξ and reduce slowly with increasing ξ and become constant.

6. In the presence of the magnetic field the shock propagates more rapidly in perfect gas. It is interesting to note that the rate of rise in the flow variables increase with the increase in the strength of magnetic field.

Acknowledgement

The authors would like to thank the referees for their valuable suggestions and comments that improved the presentation substantially.

References

[1] G. Guderley, Starke Kugelige und Zylindrische Verdichtungsstosse in der Nahe des Kugelmittelpunktes bzw der Zylinderachse, Luftfahrtforschung 19 (1942) 302–312.
[2] P. Hafner, Strong convergent shock waves near the center of convergence: a power series solution, SIAM J. Appl. Math. 48 (1988) 1244–1261.
[3] N. Manganaro, F. Oliveri, Group analysis approach in Magneto hydrodynamics: weak discontinuities in a non-constant state, Meccanica 24 (1989) 71–78.
[4] V.D. Sharma, Ch Radha, Similarity solutions for converging shocks in a relaxing gas, Internal. J. Eng. Sci. 33 (1995) 535–553.
[5] J.K. Hunter, G. Ali, Wave interactions in Magneto hydrodynamics, Wave Motion 27 (1998) 257–277.
[6] V.D. Sharma, R. Arora, Similarity solutions of strong shock waves in an ideal gas, Stud. Appl. Math. 114 (2005) 375–394.
[7] K.P. Stanyukovich, Unsteady Motions of Continuous Media, Pergamon Press, New York, 1960.
[8] R.F. Chisnell, An analytic description of converging shock waves, J. Fluid Mech. 354 (1998) 357–375.
[9] R. Lazarus, R. Richtmyer, Similarity solutions for converging shocks, Technical report LA-6823-MS, Los Alamos Scientific Laboratory, 1977.
[10] A. Ramu, M.P. Ranga Rao, Converging spherical and cylindrical shock waves, J. Eng. Math. 27 (1993) 411–417.
[11] G. Madhumita, V.D. Sharma, Propagation of strong converging shock waves in a gas of variable density, J. Eng. Mech. 46 (2003) 55–68.
[12] H.K. Sen, Structure of magneto-hydrodynamic shock waves in plasma of finite conductivity, Phys. Rev. 102 (1956) 5–11.
[13] F. De Hoffmann, E. Teller, Magneto-hydrodynamic shocks, Phys. Rev. 80 (1950) 692–703.
[14] J. Bazer, W.B. Ericson, Hydromagnetic shocks, Astrophys. J. 129 (1959) 758.
[15] V. Genot, Analytic solutions for anisotropic MHD shocks, Astrophys. Space Sci. Trans. 6 (2009) 31–34.
[16] V.P. Korobeinikov, Problems in the Theory of Point Explosion in Gases, American Mathematical Society, Providence, RI, 1976.
[17] G.B. Whitham, Linear and Non-linear Waves, John Wiley and Sons, New York, 1974.
[18] Ya. B. Zeldovich, Y.P. Raizer, Physics of Shock waves and High Temperature Hydrodynamic Phenomenon, vol. II, Academic Press, New York, 1966, pp. 785.
[19] L.D. Landau, E.M. Lifshitz, Fluid Mechanics, second ed., Pergamon Press, New York, 1987.
[20] W. Gretler, R. regenfelder, Similarity solution for laser-drivenshock waves in particle laden gas, Fluid Dyn. Res. 28 (2001) 369–382.